Review of Impulse-Radiating Antennas

Carl E. Baum[1], Everett G. Farr[2], and David V. Giri[3]

[1] Air Force Research Laboratory DEHP
3550 Aberdeen Avenue S. E.
Kirtland AFB, NM 87117-5776, USA
Tel: 1 (505) 846-5092, Fax: 1 (505) 853-3081

[2] Farr Research, Inc.
614 Paseo Del Mar N. E.
Albuquerque, NM 87123, USA
Tel: 1 (505) 293-3886, Fax: 1 (505) 323-1886
e-mail: efarr@farr-research.com

[3] Pro-Tech
1630 North Main Street, #377
Walnut Creek, CA 94596-4609, USA
Tel: 1 (925) 933-0560, Fax: 1 (925) 933-0565
e-mail: dgiri@silcon.com

Abstract

This paper reviews the progress to date concerning a special class of antennas known collectively as impulse-radiating antennas (IRAs). These are especially suited for radiating very fast pulses in a narrow beam. A fast-rising step-like signal into the antenna gives an approximate delta-function response in the far field. The frequency spectrum of the radiated pulse can be very broad (decades of band ratio). The requisite synthesis of the step-rising plane wave on the antenna aperture can be realized in various ways, including a TEM fed reflector (reflector IRA), TEM (horn) fed lens (lens IRA), and special kinds of arrays (array IRA). Such antennas have application as high-power pulse radiators, transient radars, and antennas capable of operating on many frequencies simultaneously (due to the large band ratio).

1. Introduction

Of the various types of antennas for radiating and/or receiving transient pulses, we here are concerned with a special class which are known as impulse-radiating antennas (IRAs). Basically, this type of antenna has the property that, in transmission, a fast-rising (step-like) field as a plane wave on the antenna aperture produces an impulse-like far field [2: Baum, 1989]. This can be achieved in various ways, the details of which are treated later. For large antenna apertures fed by a single source (pulser) an efficient design uses a conical transmission line terminated at and feeding a paraboloidal reflector. An alternate design has a conical transmission line (TEM horn) feeding a lens with a special resistive termination to the rear of the antenna; for large antennas the lens can be quite massive, but for small antennas this type of design is quite practical. A third approach is a transient array involving many sources feeding an aperture in a manner which purposely has continuity of current from each array element to appropriate adjacent ones so as to achieve efficient radiation, even for wavelengths large compared to element spacing (but smaller than array linear dimensions) [1: Baum, 1997].

From a historical point of view much of this technology developed out of the nuclear electromagnetic-pulse (EMP) research, specifically that associated with the large antenna and pulser systems known as EMP simulators used for testing electronic systems [1: Baum, 1978; 1: Smith and Aslin, 1978; 1: Baum, 1992]. The conical transmission waves are a comon feature. Instead of feeding into a cylindrical transmission line or distributed terminator, the conical transmission line now feeds a reflector or lens to produce a plane wave at the antenna aperture. However, such lenses have also been considered for use with EMP simulators [7: Baum, 1967]. Now, for the IRAs, one is concerned with faster rising pulses, but the antennas are smaller than typical EMP simulators. So things scale and the basic scientific concepts are, at least in part, the same.

While the motivation for developing IRA systems has often been to radiate large-amplitude, large-band-ratio (decade or more), undispersed pulses at electronic systems (and develop hardening against such environments), it is recognized that such antenna systems have various other uses as well. In the remote-sensing arena such antennas are appropriate for transient radars, including for buried targets (mines and unexploded ordnance (UXO)). Some consideration has also been given to the possible use for ionospheric research [2: Giri, 1996]. Since IRAs have such a large band ratio (ratio of upper to lower useful or roll-off frequencies), they are also being investigated for continuous-wave (CW) application, in which multiple channels/functions (communications, radar, etc.) use the same antenna [3: Farr et al, 1997].

There is now a large literature on the subject of IRAs; the present paper is intended to summarize our knowledge of this subject. There are a number of papers which review portions of this technology and these are grouped together in Section 1 of the Bibliography. With such an extensive literature it is convenient to end this paper with a bibliography which is divided according to subject areas. For reference to papers in this bibliography, the authors are preceded by a number, indicating the bibliographic section.

2. Aperture Fields for Impulse -Radiating Antennas

In the normal configuration of an IRA, a focused aperture field is turned on suddenly over the entire aperture, all at the same time. This idealized step-function time dependence is well approximated by actual sources that are currently available, although the risetime of a real source is always non-zero. So if one knows the field radiated by an ideal (step-function) source, one can convolve that result with the derivative of the actual source to obtain the actual field. Thus, we consider here the field radiated by an ideal step-function source. General papers relating to the radiation from a planar aperture appear in Section 2 of the Bibliography. The special case of a circular aperture is included as Section 9 of the Bibliography.

Consider the aperture shown in Figure 2.1. The field in the aperture is represented by $\vec{E}_t(x', y')$, with a step-function time dependence that turns on uniformly over the entire aperture. This leads to a radiated field in the far field of [2: Baum, 1989]

$$\vec{E}(\vec{r},s) = \frac{1}{2\pi r} \iint_{S_a} \gamma \left[\vec{1}_z \times \vec{E}_t(x',y',s) \times \vec{1}_R \right] e^{-\gamma R} \, dS' \tag{2.1}$$

where $\gamma = s/c$, s is the Laplace transform variable, c is the speed of light in free space, and $\vec{1}_R$ is the vector from the origin of the aperture out to the observation point. This expression simplifies under the assumption that we are looking on boresight (in the z- direction). So the radiated field on boresight in the far field simplifies to

$$\vec{E}(\vec{r},s) = \frac{1}{2\pi rc}\frac{d}{dt}\iint_{S_a} \vec{E}_t(x',y',t-r/c)\,dS' = \frac{\delta_a(t-r/c)}{2\pi rc}\iint_{S_a} \vec{E}_t(x',y')\,dx'\,dy' \tag{2.2}$$

where the $\delta_a(t)$ function is an approximate Dirac delta function whose area is unity, but whose magnitude increases proportional to r, and whose width is inversely proportional to r [2:Baum, 1989]. So the combination of $\delta_a(t)/r$ has a constant height, even in the limit as r becomes small. A clarification of the shape of the approximate delta function for various aperture fields is provided in [2: Baum, 1997a]. Other treatments of the exact shape of the delta function are found in [3: Mikheev, 1997] and [3: Skulkin and Turchin, 1997].

The tangential field in the aperture can be expressed as a field between two or more conductors with a potential difference V_o between them. Examples of two-wire and four-wire apertures are shown in Figure 2.1. It is convenient to represent the aperture field as a complex number, whose real and imaginary parts correspond to the x and y components. This complex field is expressed in terms of a complex potential function. Thus,

$$\begin{gathered} E(x,y) = E(\zeta) = E_x - jE_y = -\frac{V_o}{\Delta u}\frac{dw(\zeta)}{d\zeta} \\ \zeta = x + jy \quad , \qquad w(\zeta) = u(\zeta) + jv(\zeta) \quad , \qquad f_g = \Delta u / \Delta v \end{gathered} \tag{2.3}$$

where the complex potential function can be found in [2: Baum, 1991]. In the above formulation, Δv is the change in v around one of the conductors, and Δu is the difference in u from one conductor to the other. It was also shown that the radiated field on boresight is [2: Baum, 1991]

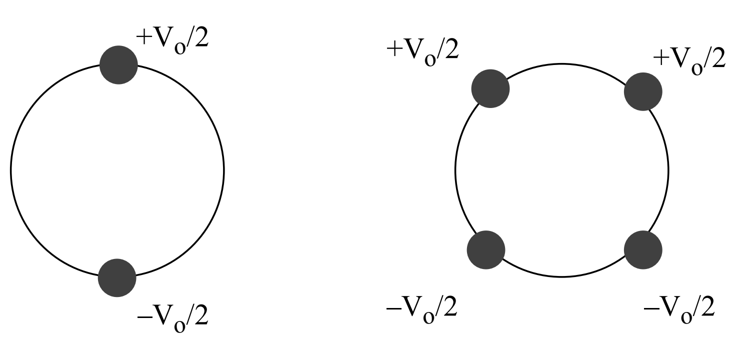

Figure 2.1. The apertures for a two-wire and four-wire configuration.

$$E^{rad}(r,t) = \frac{V_o}{r}\frac{h_a}{2\pi c f_g}\delta_a(t-r/c)$$

$$h_a = -\frac{f_g}{V_o}\iint_{S_a} E_y(x,y)\,dx\,dy = -\frac{1}{\Delta v}\oint_{C_a} v(y)\,dy \tag{2.4}$$

In the above equation, S_a is the portion of the aperture that is not blocked by the feed, and C_a is the contour around this aperture. All contour integrals are taken in the positive (counterclockwise) direction. For a two-wire aperture, shown in Figure 2.1, a high-impedance approximation was made, and the portion of the contour integral along the conducting wire was assumed very small. Under this approximation the integral is calculated as $h_a = D/2$. For the four-wire aperture case, also shown in Figure 2.1, symmetry can be used to sum two two-wire apertures, since each pair of opposing wires perturbs the field of the other pair only slightly.

Having described the impulse response on boresight, we now consider the off-boresight case. As an example, we consider the four-wire aperture of Figure 2.1. The first step is to find the fields in the aperture. To do so, we must first find the potential function that describes these fields. The potential function for the two-wire problem is well known,

$$w_2(\zeta) = 2\,j\,\mathrm{arccot}(\zeta/a) = \ln\left(\frac{\zeta/a - j}{\zeta/a + j}\right) \tag{2.5}$$

where the charge centers are located at (x=0, $y/a = \pm 1$). Here, $\zeta = x + j\,y$ is the location in the Cartesian coordinate space. This potential function was plotted in [2: Baum, 1991]. The complex potential for the four-wire case is just a sum of two two-wire potentials that have been shifted and resized, i.e.,

$$w_4(\zeta) = w_2(\sqrt{2}\zeta/a+1) + w_2(\sqrt{2}\zeta/a-1) \tag{2.6}$$

This function is complex, i.e., has both real and imaginary parts. Let us therefore set

$$u(\zeta) = \mathrm{Re}(w_4(\zeta)) \quad , \quad v(\zeta) = \mathrm{Im}(w_4(\zeta)) \tag{2.7}$$

We can plot contours of constant u and v, and these are shown in Figure 2.2 for the upper right quadrant. The conductors correspond to a contour of constant u.

To calculate the radiated field, we need the aperture fields and the normalized aperture potentials. First, we find the aperture field is

$$E_y(x,y) = \frac{-V_o}{\Delta u}\frac{\partial u(x,y)}{\partial y} \quad , \quad f_{g4} = \frac{\Delta u}{\Delta v} \tag{2.8}$$

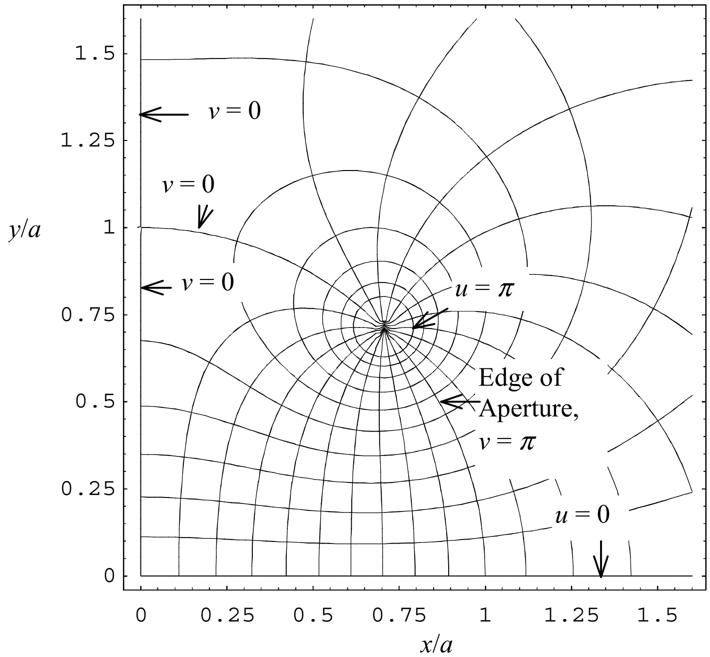

Figure 2.2. Contour map for $w_4(\zeta)$. Increments for u and v are $\pi/10$.

where V_o is the voltage difference between the top and bottom conductors. In addition, Δu is the difference in u between the two conductors, and Δv is the difference in v as one encircles one pair of positive (or negative) electrodes. Finally, the normalized aperture impedance is $f_{g4} = Z_{feed}/Z_o$, where Z_o is the impedance of free space. Note that f_{g4} is the normalized impedance for four arms and f_{g2} is the normalized impedance for two arms on opposite sides of a unit circle. Note also that for thin wire arms, $f_{g4} = f_{g2}/2$.

Next, we find the normalized potentials, which are integrals of electric field over linear paths in the aperture plane. The normalized potential for the H-plane calculation is

$$\Phi^{(h)}(x) \;=\; -\frac{1}{V_o}\int_{C_1(x)} E_y \, dy \tag{2.9}$$

where the contour $C_1(x)$ is a vertical line cut through the aperture plane, as shown in Figure 2.3. To simplify this, use the above two equations, generating

$$\Phi^{(h)}(x) \;=\; \frac{1}{\Delta u}\int_{C_1(x)} \frac{\partial u}{\partial y} dy \;=\; \frac{2}{\Delta u}\, u\left(x, \sqrt{a^2 - x^2}\right) \tag{2.10}$$

We can now calculate $u(x,y)$ as the real part of the potential function given in (2.6). Note that the value of $u(x,y)$ is a maximum when it cuts through the conductors. At this point, the value of $u(x,y)$ is $u_o = \pi f_{g2} = 2\,\pi f_{g4}$, where f_{g4} is the normalized impedance for four arms (typically

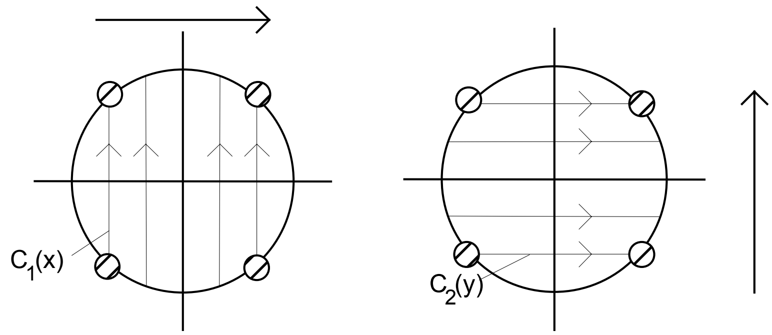

Figure 2.3. Locations of $C_1(x)$ and $C_2(y)$.

200 Ω/377 Ω). Note also that for values of x that cut through the conductors, the normalized potential is unity. This normalized potential function is plotted in Figure 2.4, on the left, for a few different values of f_{g4}.

The normalized potential for the E-plane is expressed as

$$\Phi^{(e)}(y) \;=\; -\frac{1}{V_o}\int_{C_2(y)} E_y\,dx \;=\; \frac{1}{\Delta u}\int_{C_2(y)} \frac{\partial u}{\partial y}\,dx \tag{2.11}$$

where $C_2(y)$ is a horizontal linear cut through the aperture plane, as shown in Figure 2.3. To evaluate this, we require the Cauchy-Riemann relation for analytic functions,

$$\frac{\partial u}{\partial y} \;=\; -\frac{\partial v}{\partial x} \tag{2.12}$$

We can now recast the integral as

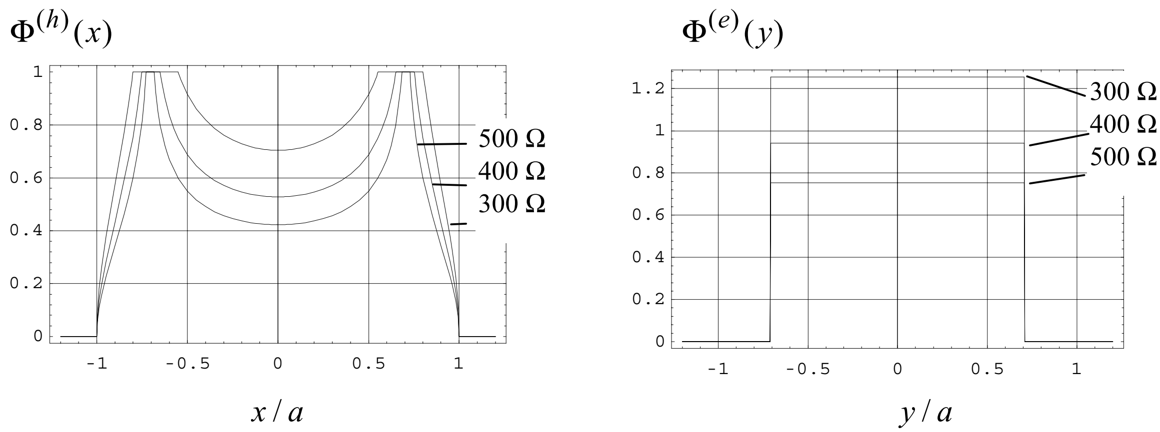

Figure 2.4. The normalized potential functions, $\Phi^{(h)}(x)$ and $\Phi^{(e)}(y)$, for a few different impedances.

$$\Phi^{(e)}(y) \;=\; \frac{-2}{\Delta u}\left[v\left(\sqrt{a^2-y^2}\,,y\right) \;-\; v(0,y) \right] \tag{2.13}$$

This is a particularly simple form, because the edges of the circular aperture are also lines of constant v. Thus, the normalized potential is evaluated analytically as

$$\Phi^{(e)}(y) \;=\; \begin{cases} 1/(2 f_{g4}) & 0 \le |y|/a \;<\; 1/\sqrt{2} \\ \quad 0 & \text{else} \end{cases} \tag{2.14}$$

We have plotted the normalized potentials for a few impedances in Figure 2.4, on the right. Note that our theory predicts an abrupt discontinuity in $\Phi^{(e)}(y)$ near the wires. In fact, there is actually a more smooth transition between the two values, but if the wire is thin, this is an excellent approximation.

With the normalized potentials calculated, we can now calculate the radiated field as a function of angle off boresight in the H and E-planes. The aperture field is created by a step voltage of magnitude V_o across the aperture, so from [3: Farr, 1993] we find

$$\begin{aligned} \vec{E}_{step}{}^{(h)}(r,\theta,t) \;&=\; \vec{1}_y \,\frac{-V_o}{r}\,\frac{\cot(\theta)}{2\pi} \quad \Phi^{(h)}\!\left(\frac{ct}{\sin(\theta)}\right) \\ \vec{E}_{step}{}^{(e)}(r,\theta,t) \;&=\; \pm\,\vec{1}_\theta \,\frac{-V_o}{r}\,\frac{1}{2\pi\sin(\theta)} \;\; \Phi^{(e)}\!\left(\frac{ct}{\sin(\theta)}\right) \end{aligned} \tag{2.15}$$

This completes the calculation of the step response radiation for a full 4-wire aperture, while it is still focused. To find the response to a standard Gaussian pulse, we convolve the above step response with the derivative of the time domain driving voltage.

3. IRA Performance in Transmission and Reception

In order to define figures of merit in the time domain, we must express the radiated and received fields in terms of the incident voltage (in transmission) and the incident field (in reception). The diagrams showing the relevant quantities are shown in Figure 3.1. Note that there is a resistive load that is matched to the characteristic impedance of any feed transmission line attached to the antenna port. (This will also be matched to the IRA feed, which is itself a conical transmission line.) This is analogous to the use of scattering parameters in circuit theory. Papers relating to transient gain, figures of merit, and reciprocity appear in Section 6 of the Bibliography.

First we describe the relevant equations in the frequency domain. Because of the resistive termination matched to the feed line, which in turn is matched to the antenna, in transmission $V_t(t)=V_s(t)/2$. Instead of referring to port voltages, we will refer to voltage waves, in the spirit of S-parameters in microwave theory. Thus, the transmitted and radiated fields are [6: Baum, 1991]

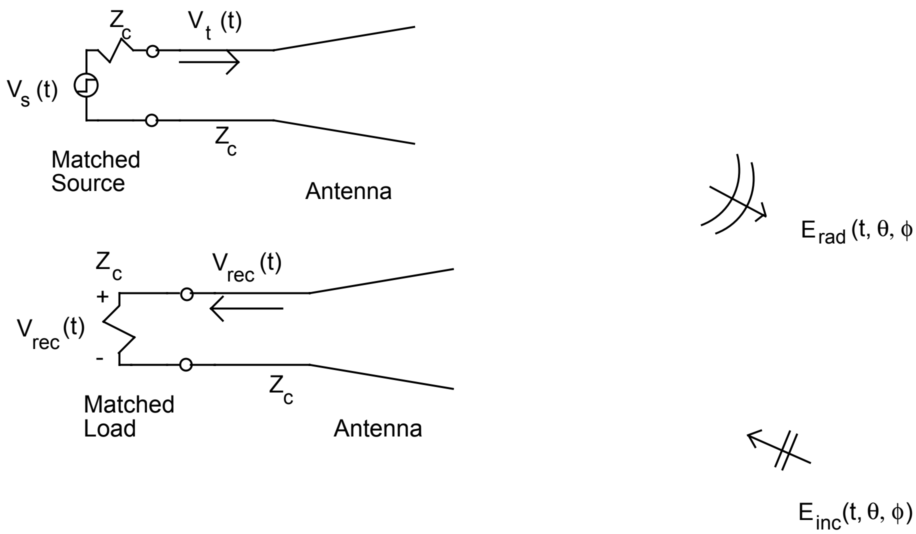

Figure 3.1. A transient antenna in transmit mode (top) and receive mode (bottom).

$$
\begin{aligned}
&\text{Transmit} && \tilde{\vec{E}}_{rad}(\vec{r},s) = \frac{e^{-\gamma r}}{r}\,\tilde{\vec{F}}_t(\vec{1}_r,s)\,\tilde{V}_t(s) \\
&\text{Receive} && \tilde{V}_{rec}(s) = \tilde{\vec{h}}_t(\vec{1}_i,s) \mathbin{\overset{\circ}{\cdot}} \tilde{\vec{E}}_{inc}(s) \\
&\text{Reciprocity} && \tilde{\vec{F}}_t(\vec{1}_r,s) = \frac{s\mu_o}{2\pi Z_c}\,\tilde{\vec{h}}_t(-\vec{1}_r,s)\,, \qquad \vec{1}_i \cdot \tilde{\vec{h}}_t = 0 \\
& && \overleftrightarrow{1}_r = \overleftrightarrow{1} - \vec{1}_r\,\vec{1}_r\,, \qquad \overleftrightarrow{1} = \vec{1}_x\,\vec{1}_x + \vec{1}_y\,\vec{1}_y + \vec{1}_y\,\vec{1}_y\,,
\end{aligned}
\tag{3.1}
$$

where $\vec{1}_r$ is the direction of radiation. The time domain analogs of these equations are

$$
\begin{aligned}
&\text{Transmit} && r\,\vec{E}_{rad}(\vec{r},t) = \left[\int_0^t \vec{F}_t(\vec{1}_r,t')\,dt'\right] \circ \frac{dV_t(t-r/c)}{dt} \\
&\text{Receive} && V_{rec}(t) = \vec{h}_t(\vec{1}_i,t) \mathbin{\overset{\circ}{\cdot}} \vec{E}_{inc}(t) \\
&\text{Reciprocity} && \vec{F}_t(\vec{1}_r,t) = \frac{\mu_o}{2\pi Z_c}\frac{d}{dt}\vec{h}_t(-\vec{1}_r,t)
\end{aligned}
\tag{3.2}
$$

where the $\circ$ operator indicates a convolution and the dot product convolution operator $\overset{\circ}{\cdot}$ implies a sum of the convolution of each component of the vectors. Note that the units of $\vec{h}(t)$ are meters/second. Note also that the function $\int_0^t \vec{F}_t(\vec{1}_r,t')\,dt'$ is the step response in transmission, which has been characterized for reflector IRAs (earlier in this paper) and for TEM horns by [4: Farr and Baum, 1992]. Finally, note that $\vec{h}_t(\vec{1}_t,t)$ is just the step response in transmission times some constants.

There is a general class of figures of merit for time domain radiators, which we refer to as FM. To find the FM, we drive the antenna with a standard waveshape, such as the integral of a Gaussian (in transmission) or a Gaussian (in reception). Because of the above reciprocity relationship in the time domain we can establish a correlation between the transmit and receive cases. The FM is defined in terms of norms as

Transmission Reception

$$FM(\theta,\phi) = \frac{1}{\sqrt{f_g}} \frac{\left\| V_{rec}(t) \right\|}{\left\| \vec{E}_{inc}(\theta,\phi,t) \cdot \vec{1}_e \right\|} , \quad FM(\theta,\phi) = \lim_{r\to\infty} \frac{2\pi c\sqrt{f_g}\left\| r\,\vec{E}_{rad}(\theta,\phi,t)\cdot\vec{1}_e \right\|}{\left\| dV_{inc}(t)/dt \right\|} \tag{3.3}$$

where $\vec{1}_e$ is one of two orthogonal polarizations. The above two definitions are guaranteed to be equal if the driving voltage waveshape in transmission is the integral of the incident electric field in reception. One can think of the norm of a function as one of several commonly used characteristics of a time domain function, such as the peak of the function (∞-norm), the integral of magnitude of the function (1-norm), or the square root of " energy" in the function (2-norm). By way of review, a norm must satisfy three fundamental properties,

$$\left\| f(t) \right\| \begin{cases} = \ 0 & \text{iff}\, f(t) \equiv 0 \\ > \ 0 & \text{otherwise} \end{cases} , \ \left\| \alpha\, f(t) \right\| = |\alpha| \left\| f(t) \right\| , \ \left\| f(t) + g(t) \right\| \le \left\| f(t) \right\| + \left\| g(t) \right\| \tag{3.4}$$

A commonly used norm is the p-norm, which is defined as

$$\left\| f(t) \right\|_p \equiv \left(\int_{-\infty}^{\infty} |f(t)|^p \, dt \right)^{1/p} , \qquad \left\| f(t) \right\|_\infty \equiv \sup_t |f(t)| , \tag{3.5}$$

The choice of the norm will usually be tied to the experimental system. Thus, if a transient radar receiver responds to the peak magnitude of the received signal, then one should use the ∞-norm in the figure of merit definition.

Another useful way of looking at the parameters of an IRA is to consider the relationship of the impulse response, $\vec{h}_t(\theta,\phi)$ to the standard definitions of gain and effective area. We begin with the standard expressions in the frequency domain. Thus, the received power is

$$\tilde{P}_{rec} \ = \ \tilde{A}_{eff} \ \tilde{S}^{(inc)} \tag{3.6}$$

where $\tilde{S}^{(inc)}$ is the incident power density in W/m^2 and A_{eff} is the effective aperture. Gain is related to effective aperture by

$$\tilde{A}_{eff} = \frac{\lambda^2}{4\,\pi}\,\tilde{G} \tag{3.7}$$

Combining the above two equations, we have

$$\tilde{P}_r = \frac{\lambda^2\,\tilde{G}}{4\,\pi}\,\tilde{S}^{(inc)} \tag{3.8}$$

Take the square root, and recast into voltages

$$\frac{\tilde{V}_r}{\sqrt{Z_c}} = \frac{\lambda\,\sqrt{\tilde{G}}}{2\,\sqrt{\pi}}\,\frac{E^{(inc)}}{\sqrt{Z_o}} \tag{3.9}$$

where Z_o is the impedance of free space, and Z_c, the feed or input impedance, is assumed a positive constant. . Thus, the final result in the frequency domain is

$$\tilde{V}_r = \frac{\lambda\,\sqrt{\tilde{G}\,f_g}}{2\,\sqrt{\pi}}\,\tilde{E}^{(inc)} \tag{3.10}$$

where $f_g = Z_c/Z_o$.

Let us now compare the above equation to one that we have been using in the time domain, where we restrict the consideration to boresight for which symmetry allows us to scalarize the problem as

$$\tilde{V}_r(t) = h_t(t) \circ \tilde{E}^{(inc)}(t) \tag{3.11}$$

We routinely have already measured $h_t(t)$, so we just have to rescale to get gain. Converting this to the frequency domain, we have

$$\tilde{V}_r(j\omega) = \tilde{h}_t(\omega)\;\tilde{E}^{(inc)}(j\omega) \tag{3.12}$$

Now compare (3.10) and (3.12), to get

$$\boxed{\tilde{G}(\omega) = \frac{4\pi}{\lambda^2}\,\frac{|\,\tilde{h}_t(j\omega)\,|^2}{f_g} = \frac{4\pi f^2}{c^2}\,\frac{|\,\tilde{h}_t(j\omega)\,|^2}{f_g}} \tag{3.13}$$

We can use this to scale our $h_t(t)$ waveforms to get a frequency-domain gain. Note the similarity between (3.7) and (3.13). The implication is that the effective aperture as a function of frequency is $|h_t(j\omega)|^2/f_g$, which is a rather simple and pleasing result.

There is a drawback with this definition, in that it does not take into account dispersion, or time delay. If different frequencies have different time delays (as happens on more conventional antennas), the received pulse will not be clean. But the above definition of gain does not take this into account. Thus, using this definition of gain, two antennas with the same gain can have very different peak radiated E-fields.

4. Reflector IRA

In Section 2 we described the impulsive portion of the radiation from a focused aperture antenna on boresight. Here, we extend that theory to find a more complete waveform of a reflector IRA on boresight. Papers relating to reflector IRAs appear in Section 3 of the Bibliography.

Consider what happens when a step voltage drives the IRA shown in Figure 4.1. There is a prepulse for a time $2F/c$, where F is the focal length of the reflector. This is due to the direct radiation of the currents on the feed arms. The shape of this prepulse is a step function, similar to the driving voltage. In Section 2 we saw that the impulsive portion of the radiated field is an approximate delta function, so let us consider a radiated waveform shown in Figure 4.2. The area of the impulse is known from Section 2. Furthermore, it is possible to calculate the direct radiation from a conical feed by using various stereographic projections. If the area under the prepulse is equal to the area under the impulse, then the tail portion of the waveform can be made small with proper tuning of the matching circuit. (Additional characterization of the postpulse (tail) is in [3: Giri and Baum, 1994 and 1997].)

We calculate now the magnitude of the prepulse. It is simplest to calculate this for the geometry of two circular cones, as shown in Figure 4.3. If one were interested in a feed consisting of flat plates (either facing or coplanar), then for high impedances (small α) the results for the circular cones describe the plate geometries of angular width 4α as well. For lower impedances, more exact expressions are available [3: Farr and Baum, 1992].

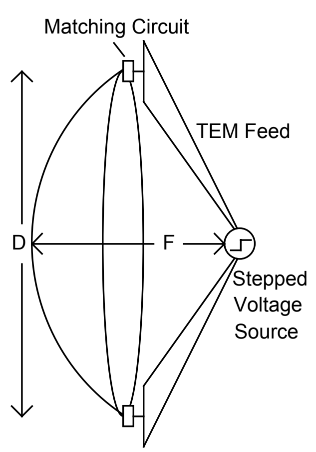

Figure 4.1 A reflector IRA.

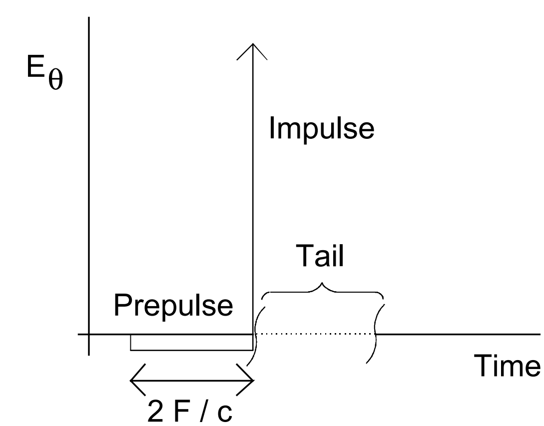

Figure 4.2. Approximate waveform of a Reflector IRA

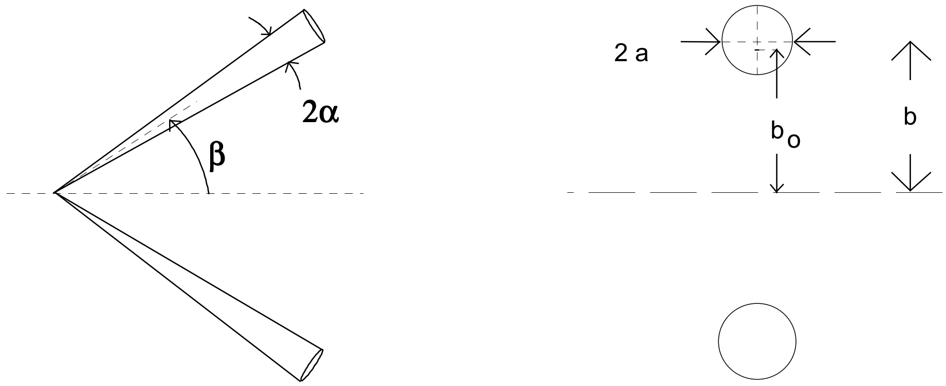

Figure 4.3. Circular cone feed of a reflector IRA (middle), and projection of the conical feed onto a plane (right).

It is now necessary to project the spherical geometry of the circular cones onto a planar surface. In order to do so, we invoke the usual stereographic projection. Thus, the polar coordinates in the projection plane are

$$x = 2F \cos(\phi) \tan(\theta/2) \quad , \quad y = 2F \sin(\phi) \tan(\theta/2) \tag{4.1}$$

The projection of the spherical cone generates a cylindrical structure whose cross-section is two circles with half height b and radius a such that

$$b = \frac{2F\sin(\beta)}{\cos(\alpha)+\cos(\beta)} \quad , \qquad a = \frac{2F\sin(\alpha)}{\cos(\alpha)+\cos(\beta)} \tag{4.2}$$

where a and b are as shown in Figure 4.4. It is simple to find the electric field at the center of the projected structure [3: Farr and Sower, 1995]. Thus, we find the backward radiated field (forward as far as our antenna is concerned) to be

$$E_\theta = -\frac{V}{r_o} \frac{\cos(\alpha) - \cos(\beta)}{\pi f_g \tanh(\pi f_g) \sin(\beta)} \tag{4.3}$$

This is just what we need for calculating the ratio of the prepulse area to the impulse area. The impulse area is found by integrating (3.10) with respect to time. The prepulse area is found by multiplying (4.3) by $2F/c$, the round trip transit time of the feed. The ratio of the prepulse area to the impulse area is found to be

$$\left|\frac{A_p}{A_i}\right| = \frac{4(F/D)\left[\cos(\alpha) - \cos(\beta)\right]}{\tanh(\pi f_g) \sin(\beta)} \tag{4.4}$$

If this ratio is approximately equal to unity, then the two areas are equal. For the types of parameters in which one is typically interested ($F/D = 0.4$, $Z_{feed} = 400\ \Omega$), the areas are equal to better than 1%. Thus, a reasonable expression for the on-boresight radiated field in response to a step-function excitation is

$$E(r,t) = \frac{V_o}{r}\frac{D}{4\pi c f_g}\left[\frac{c}{2F}\left[-u(t) + u(t - 2F / c)\right] + \delta_a(t - 2F / c)\right] \tag{4.5}$$

With a time-varying source, with voltage $V(t)$, the expression is simply

$$E(r,t) = \frac{D}{4\pi r c f_g}\left[\frac{c}{2F}\left[-V(t) + V(t - 2F / c)\right] + \frac{dV(t - 2F / c)}{dt}\right] \tag{4.6}$$

Of course, this expression makes use of a number of assumptions, including the use of an ideal matching circuit at the boundary between the feed and reflector. A second assumption is that the aperture blockage is small (valid for thin feed projections). Nevertheless, it is very helpful that such a simple result is available for such a complex structure.

Note that the impulsive portion of the above response was calculated with the assumption that the feed is long. This is an unnecessary constraint, as shown by [3: Farr and Baum, 1992]. It is shown there that a reflection off a paraboloidal reflector produces a flat phase front with the same aperture field distribution as an infinitely long cylindrical transmission line (TEM mode), and is exactly expressed by the usual stereographic transformation (with minus sign, reflector transformation).

Note also that the feed arms in a reflector IRA are normally terminated in the characteristic impedance of the feed arms, at a point near the reflector. This serves several purposes. First, it drains the high-voltage charge that accumulates on the feed arms. Second, it provides low-frequency electric and magnetic dipoles that are approximately balanced. This leads to a low-frequency pattern of 1+cos(θ), pointing in the correct (boresight) direction. Finally, because the feed is terminated to the reflector in the feed impedance, one can achieve a very good match to the input impedance. Thus, one can get a very flat TDR with this design.

Having described the response of a generic reflector IRA, we now consider a specific example, which was built by D. V. Giri [3: Giri *et al*, 1997]. A photograph of the system is shown in Figure 4.4. The system consists of a parabolic reflector illuminated by a pair of conical 400 ohm TEM feeds, which are electrically connected near the feed apex. Each of these twin 400 ohm feeds incorporate a very low inductance ~100 pF series ceramic capacitors in each conductor, near the feed apex. The capacitors are then switched by a low inductance, high pressure (~100 atm), hydrogen gas spark gap. The resulting double exponential pulse has a 10-90% risetime of about 100 ps and an e-fold decay of about 20 ns. The system is capable of burst mode operation at up to 200 Hz.

Representative waveforms measured on and near boresight at a distance of 304m is shown in Figure 4.5, [3: Courtney et al, 1995] and other performance parameters are shown in Table 4.1.

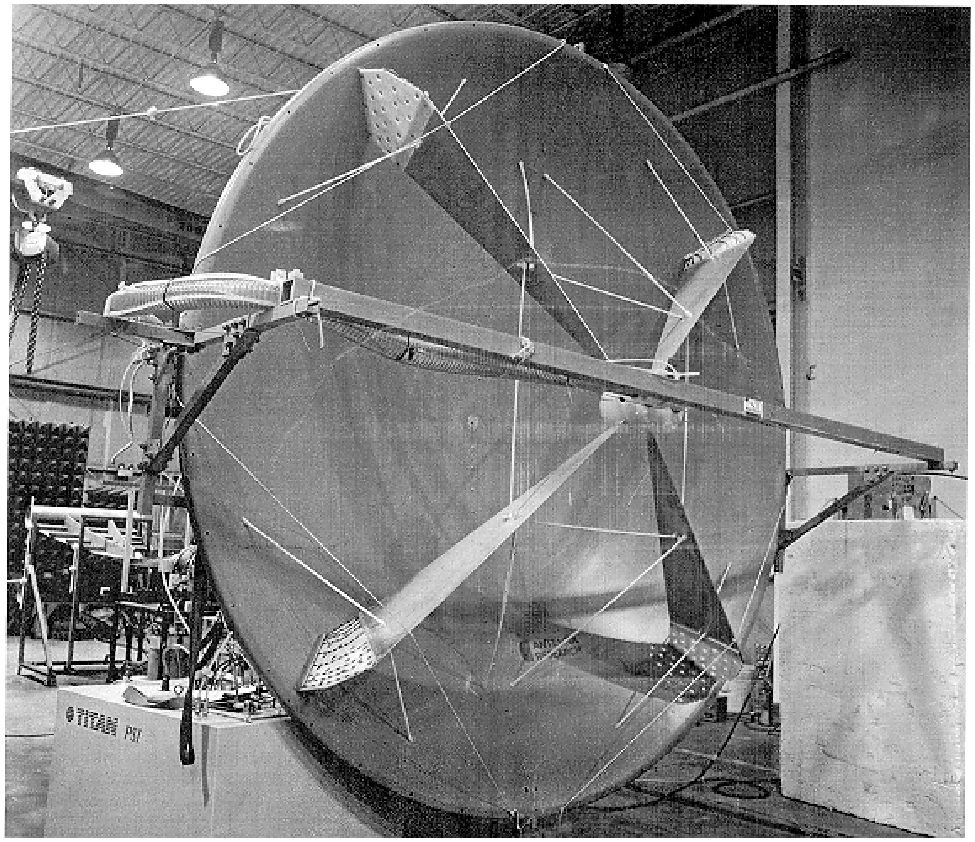

Figure 4.4. The 12-foot diameter reflector IRA built by D. V. Giri.

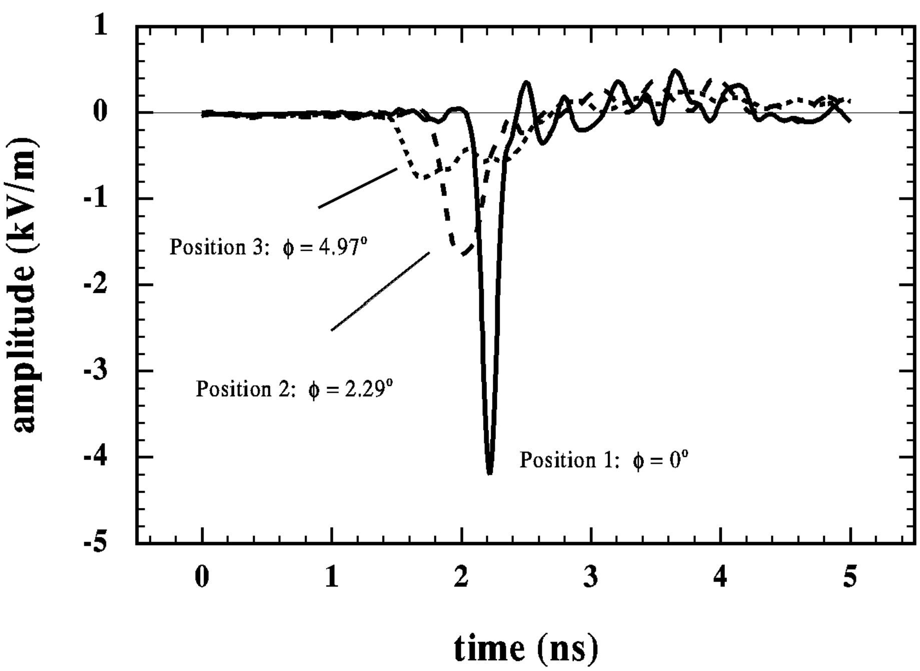

Figure 4.5 Measured temporal electric field at r = 305m, at angle of 0, 2.29, and 4.97 degrees off-boresight in the H-plane.

Table 4.1 Summary of the Reflector IRA Measurements

Physical Quantity	Numerical Value
Peak electric field on bore sight at r = 305 m	4.2 kV/m
Bore sight electric field (10-90%) risetime, r = 305 m	99 ps
Bore sight impulse duration (FWHM), r = 305 m	130 ps
Bore sight electric field spectrum, r = 305 m	< 12 dB variation over 50 MHz - 4 GHz
Main beam scan: FWHM θ - beam width FWHM ϕ - beam width	 -1.77^o, $+1.45^o$ -0.98^o, $+2.31^o$
Azimuthal, or H-plane pattern: FWHM ϕ - beam width -3 dB peak power beam width	 3.18^o 1.80^o
Incident electric field at the center of the dish (10-90%) risetime	~ 34 kV/m 126 ps*
V(far) = r E(far)	~ 1281 kV
*(instrumentation limited sensor ~ 100 ps, scope ~ 56 ps)	

The key Elements of the system include

- Impulse Radiating Antenna (IRA) of the type proposed by Baum
- An electromagnetic lens to ensure near ideal spherical TEM wavelaunch
- Use of plastics matched to the dielectric constant of the insulating oil
- A high pressure (~ 100 atm.), low inductance, rep-rate, H_2 as spark gap
- Ceramic capacitors incorporated into the TEM feed line profiles
- True differential charging and switchout of the capacitor/switch elements
- Long burst (> 500 pulses), 200 Hz rep-rate operation
- Computer based, fiber optic isolated control system

5. Lens IRA

A lens IRA is basically a TEM horn with a lens at the aperture to straighten out the spherical TEM wave on the conical transmission line into a plane wave at the end (aperture). Having said that, there are many details to consider. Figure 5.1 gives a general picture of this type of IRA. More concerning the lenses is given in Section 7. Section 4 of the bibliography (as well as selected papers in other sections) gives a more extensive discussion of this type of IRA.

TEM horns have a long history [5: Baum, 1967; 4: Shaubert, 1977; 4: Kanda, 1983] for various applications (EMP simulators, communications antennas, measurements). For IRA application, however, it is only in the limit of small divergence angle of the horn (or sufficiently long horn for given aperture dimensions and desired narrow radiated pulse width) that a TEM horn can be thought of as an IRA [4: Farr and Baum, 1992]. In general a lens is required to make the antenna fields into a plane wave at the aperture.

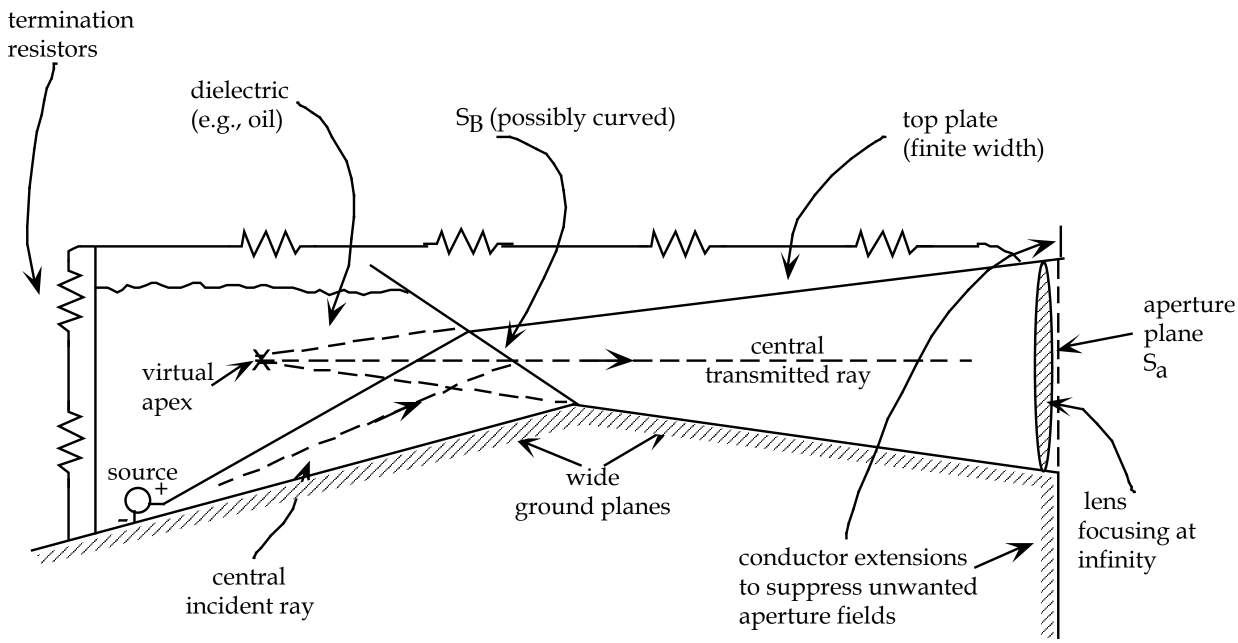

Fig. 5.1 Lens IRA for High-Power Application.

For small antennas, this type of antenna is a practical choice for an impulse radar [2: Farr and Frost, 1995]. It has been noted [2: Farr, 1995] that an optimum feed impedance for a lens IRA (differential) is around 200 Ω, similar to that for a reflector IRA (differential).

Part of a lens-IRA design concerns the termination of the conical transmission line in an optimal manner. As discussed in [4: Baum, 1995], a resistive termination near the aperture is not good because it makes the low-frequencies radiate preferentially in the backward direction (opposite to the early-time or high-frequency radiation). As indicated in fig. 5.1 [2: Baum, 1995a], this problem is overcome by routing the resistive termination around behind the horn, thereby reversing the low-frequency magnetic-dipole moment $\vec{m}$, which together with the corresponding electric-dipole moment $\vec{p}$, makes the low-frequency radiation in the $\vec{p} \times \vec{m}$ direction be in the forward direction. Detailed calculations [2: Vogel, 1996 and 1997] show how to position the resistors and adjust the resistances so as to make

$$|\vec{p}| = \frac{|\vec{m}|}{c} \tag{5.1}$$

and make the backward low-frequency radiation have a null with a cardiod pattern [6, Baum, 1991].

Lens IRAs can be designed for differential or single-ended pulsers. For high-voltage applications, single-ended pulsers are more commonly available. In this case the TEM horn takes the form of a single conical plate with apex on a large ground plane, with pulser feeding through the ground plane at the apex. As indicated in Fig. 5.1, as one goes from the aperture back toward the source, the fields can become so large that electrical breakdown is a significant problem. One can use a high-dielectric-strength gas (e.g., SF_6), but as spacing becomes smaller even this dielectric strength can be exceeded. Then one might use transformer oil in the region nearest the source. This has a lower wave impedance due to its higher relative permitivity, $\varepsilon_r \simeq 2.25$. One can partially compensate for this by bending the conical transmision line as it passes through the oil/gas interface sloped at the Brewster angle, giving no refletion of the important vertically polarized electric-field component (with reference to fig. 5.1). Furthermore, the characteristic impedances of the two conical transmission lines are more closely matched.

The oil/gas interface can be maintained by a plastic (e.g., polyethylene) with the same dielectric constant as the oil. Furthermore, as discussed in detail in [2: Baum, 1995a], this interface can be treated as a lens surface. In order to make the wave launched on the second horn (gas section) approximate a spherical wave (minimum dispersion) originate from the virtual apex, the interface can be appropriately curved to remove astigmatism. This required different curvatures in E and H planes. An interesting case has no curvature (flat) in the H plane giving a surface shaped approximately as a circular cylinder (axis in H plane). A prototype involving such considerations has been constructed [4: Wells et al, 1997].

At the aperture plane one can install a lens (approximate) to convert the spherical wave to a plane wave of the type discussed in [7: Baum, 1967]. While there are reflections at the two lens surfaces, the transmitted field is reduced by only a few percent for plastic/oil lenses of relative dielectric constant discussed previously. However, as the lens IRA becomes larger, the lens volume and associated mass and weight grow proportional to the cube of the linear dimensions for a given antenna shape.

6. Array IRA

An array IRA is basically a set of pulsed sources on a plane (or other shape if desired), triggered in such a way as to produce a plane wave on the antenna aperture. This is then a timed array (analogous to a phased array). One of the advantages of such an IRA is the possibility of electronic beam stearing. For some applications the rapid-steering capability may be sufficiently important so as to offset the increased complexity. Another motivation for such an antenna concerns high-power application. As one increases the total voltage across the array the rise-time limitations of a single switch (such as for a reflector or lens IRA) become severe, leading to the desirability of replacing the single switch by an array (series/parallel) of switches operating at lower voltages. Of course, multiple switches bring with them the problem of switch jitter (which should be small compared to the switch rise time (e.g., 100 ps).

An interesting way to construct such an array is from a set of TEM horns (small conical transmission lines) connected together so that for wavelengths large compared to the individual elements, currents can flow from one element to the next [5: Baum, 1967]. As indicated in Fig. 6.1, this produces a large average electric field across the aperture giving an efficient radiator for such low frequencies [5: Baum, 1970]. Originally such arrays were designed for various types of

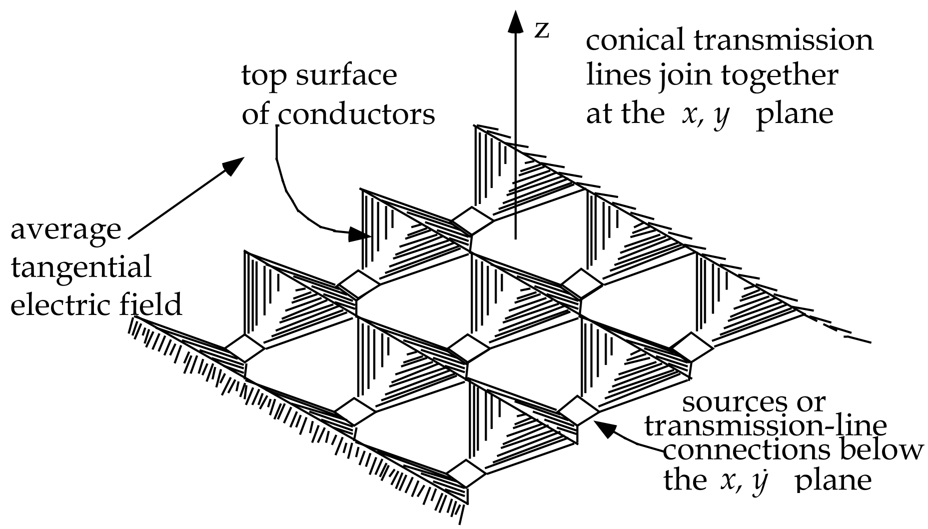

Fig. 6.1 Non-Planar Conical Transmission Lines.

EMP simulators [1: Baum, 1978, 1992]. More recently [1: Baum, 1997] attention has been given to arrays for radiating narrow high-amplitude transient pulses. (See Section 5 of the bibliography.)

Here w_1 and w_2 give the cross-section dimensions of an array unit cell. This ratio can be varied for impedance purposes. The length ℓ of the conical transmission lines forming the unit cells can also be varied so as to optimize the high-frequency performance. For flat unit cells ($\ell = 0$) the effective rise time t_1 has $ct_1 \simeq 1$ for $w_1 \simeq w_2$. For infinitely long launcher elements ($\ell \to \infty$) one has $ct_1 \simeq 0$ (perfect switch providing step-function pulse assumed) for broadside excitation (all switches closed simultaneously). This leads to the concept of a dispersion distance or time which gives the difference in arrival time of the field on each unit cell of the aperture plane as

$$
d_e^{(1)} = ct_e^{(1)} = \left[\ell^2 + \frac{w_1^2 + w_2^2}{4}\right]^{\frac{1}{2}} - \ell \to \frac{w_1^2 + w_2^2}{8\ell} \quad \text{as} \quad \frac{\left[w_1^2 + w_2^2\right]^{\frac{1}{2}}}{\ell} \to \infty \tag{6.1}
$$

There is also another dispersion associated with the transverse dimensions of the unit cell for the case that the beam angle θ_1 (measured away from array normal) varies away from zero. If w is the width of the unit cell in the direction of wave propagation across the array this space/time difference (dispersion) is

$$d_e^{(2)} = ct_e^{(2)} = w \sin(\theta_1) \tag{6.2}$$

If one wishes to scan the array over

$$0 \le \theta_1 \le \theta_1^{(\max)} \tag{6.3}$$

then this specifies

$$d_e^{(2,\max)} = w^{(\max)} \sin\left(\theta_1^{(\max)}\right) \tag{6.4}$$

where *w* can achieve a maximum value of

$$w^{(\max)} = \left[w_1^2 + w_2^2\right]^{\frac{1}{2}} \tag{6.5}$$

for particular choices of the aximuthal scan angle ϕ_1. There is not much point in making $d_e^{(1)} << d_e^{(2)}$. One may choose these two to be comparable for an appropriate design compromise.

With some choice of $\theta_1^{(\max)}$ and some desired small dispersion, the array-element (unit-cell) dimensions are constrained. The length ℓ is limited so that a ray path from each source is kept within the horn. The cross-section dimensions are limited by $w^{(\max)}$. For smaller dispersion or faster effective risetime one needs more array elements to fill a given array area. This represents a significant design tradeoff.

The design in fig. 6.1 is for a single polarization. Dual polarization can be achieved by the design in Fig. 6.2 with two TEM horns in each unit cell. Various other designs for single or dual polarization are also achievable based on regular parallelograms that divide up a plane (equilateral triangle, square, regular hexagon) [1: Baum, 1997; 5: Baum, 1970].

As with reflector and lens IRAs, an array IRA can also be designed to meet the balanced $\vec{p} \times \vec{m}$ condition (e.g., (5.1)), so as to enhance the low-frequency radiation as a cardiod pattern peaked in the forward direction [5: Baum, 1993]. Figure 6.3 illustrates a technique in which a loop with terminating resistors *behind* the array is used to produce the requisite magnetic-dipole moment.

The array IRA is the most recently investigated type of IRA and the most complex type. Accordingly, it is the least well understood and research is continuing. Numerical computations [5: McGrath, 1996] have begun and show promise for a better future understanding and design of prototype arrays.

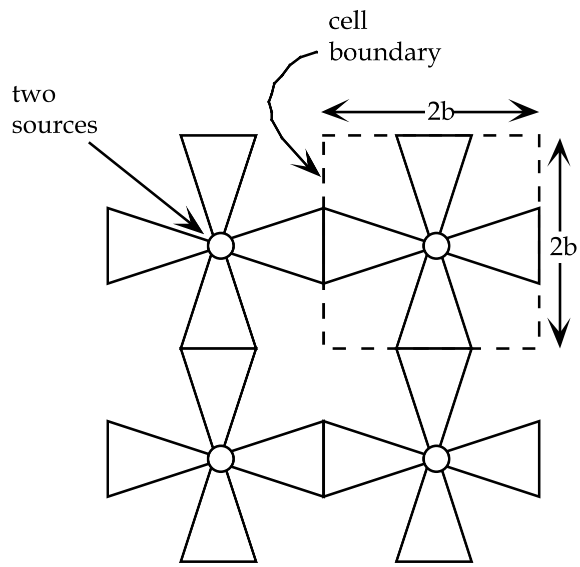

Fig. 6.2 Square Cell Geometry for Dual Polarization (Front View).

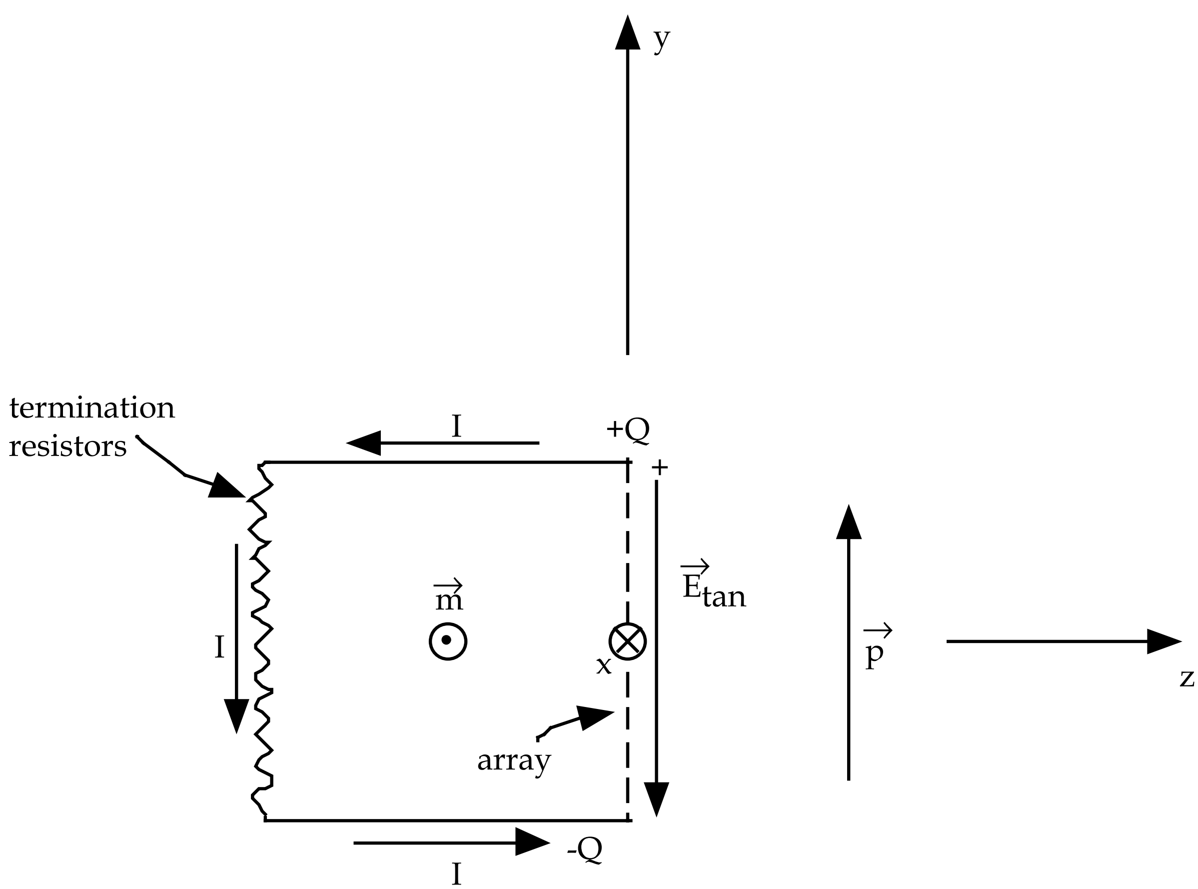

Fig. 6.3 Additions to Array for Balanced Low-Frequency Electric- and magnetic-Dipole Moments (Side View).

7. Transient Lenses

Lenses can be included as parts of various types of IRA systems. Besides straightening out the wave exiting a conical TEM waveguide (horn) as in a lens IRA (Section 5), lenses are used to redirect TEM waves (such as on coaxial waveguides) from one direction to another (bending lens) and/or between plane and spherical TEM waves. Note that the transient lenses used for this purpose are quite different, in general, from narrowband lenses (optical or microwave). In particular they need to have low dispersion for passing pulses with low distortion, and they often are constructed with transmission-line conductors passing through them and matching to TEM waveguides on both sides. In some cases the lenses and interface surfaces also need to withstand extremely high electric fields. These lenses come in two general kinds to which we can refer as approximate and exact.

7.1 Approximate lenses

These are often constructed with some uniform dielectric such as polyethylene or transformer oil. Transit times through the lens are preserved for the various ray paths between the appropriate planar and/or spherical surfaces on both sides of the lens. However, some reflections at the lens surfaces are accepted in the interest of simplicity. Essentially the differential impedances along a duct [8: Baum and Stone, 1991] are not constant. However, for not-too-large variations in the relative dielectric constant ε_r (about 2.25 for polyethylene and transformer oil) the performance is acceptable in some applications.

Section 7 of the Bibliography lists the various papers on this subject. In particular the design in [7: Baum et al, 1993] has been successfully incorporated in the launch onto the conical transmission line in a large reflector IRA [3: Giri et al, 1997; 3: Giri and Baum, 1977]. Other designs are under study.

7.2 Exact lenses

Ideally, one would like to have the wave transitioned between TEM waveguides with *no* distortion. How to do this, and the extent to which this can be done is the synthesis problem for such lenses. This can be viewed in two ways as discussed in [8: Baum and Stone, 1991].

One fundamental approach involves a differential geometric scaling from some simpler problem (the formal problem) with a known TEM solution (say an inhomogeneous TEM plane wave) in some as yet unspecified u_1, u_2, u_3 orthogonal currilinear coordinate system (the formal system) initially regarded as Cartesian. Then regarding the u_n coordinates more generally one asks what coordinate systems give acceptable permeability $\overleftrightarrow{\mu}(\vec{r})$ and permittivity $\overleftrightarrow{\varepsilon}(\vec{r})$ tensors to support the TEM wave (the real fields) in the now curved coordinates. In addition, this "lens region" generally needs to be matched to other regions with other TEM waves (planar/spherical) on appropriate boundary surfaces.

A second approach uses the duct concept mentioned previously. Transit times between appropriate surfaces are made the same for all rays. A duct surrounding each ray is also made to have the same impedance all along the ray (differential impedance matching). The first approach implies the conditions mentioned above, but the second approach has allowed some solutions with special kinds of anisotropic media involving metal sheets.

The earlier papers on this subject are summarized in [8: Baum and Stone, 1991]. Since then more progress has been made as indicated by the papers in Section 8 of the Bibliography. In particular in recent years research has concentrated on purely dielectric exacct lenses. This is related to the difficulty of constructing magnetic materials with frequency independent (and lossless) permeability over frequency ranges of interest (say 10s of MHz to 10s of GHz, depending on specific application). Various dielectrics are dispersionless (for practical purposes and over not-too-large lengths) over such frequencies. Of particular note is the discovery of a class of solutions for a dielectric bending lens [8: Baum, 1996d]. This has the potential for being quite practical and early experiments are reported [8: Bigelow and Farr, 1998].

8. Some Related Matters

Impulse-radiating antennas have been developed with practical applications in mind involving impulse-like fields in the far field. At the same time various investigators have been exploring special kinds of pulsed electromagnetic waves for special properties (narrow beams, near field conditions, etc.). A selected set of references has been included for the reader in Section 10 of the Bibliography. One of the limitations of some of these waves is their mathematical idealization involving the use of frequencies tending to infinity with significant amplitudes, a condition limited by real equipment. Nevertheless, these results can shed some insight into what is (or is not) achievable in a pulse-radiating antenna.

9. Concluding Remarks

Recent years have shown much progress in the design of impulse-radiating antenna for various applications. There is ongoing research on multifunction IRAs [3: Farr et al, 1997] in which a single antenna handles multiple signals for communications, radar, and/or electronic warfare. This involves multiple frequencies, possibly broadband pulses, polarization diversity, transmit and receive. Furthermore, the beamwidth may be variable by defocusing the antenna by moving the feed point relative to the reflector, or by altering the reflector shape (in this case the antenna not being strictly an IRA). The array IRA also needs much more development for practical implementation.

Besides strictly antenna issues, there are pulse-power issues for high-power IRAs operating in pulse mode. Fast-rising high-voltage switching of pulses into the antenna can be of the order of 6×10^{15} V/s [2: Lehr et al, 1997]. To extend this performance one may investigate multichannel switching or multiple switches (which now required small switch jitter) as in an array (Section 6). In addition there are design problems in avoiding electrical breakdown on the antenna involving high-dielectric-strength materials. The exact lenses (Section 7.2) also need to be realized in a good approximation using graded dielectrics which can also withstand high fields.

There are also mechanical issues requiring attention. Particularly near the feed point (apex of the conical transmission line) the conical conductors and connections can be quite delicate considering their connection to large antenna structures which transmit large forces. These forces need to be relieved so as not to be transmitted to the apex. For some applications weight can be a problem and one needs to avoid massive dielectric lens-like structures in such cases.

10. Bibliography

The various Notes cided in the bibliography are available from the authors or the editor C. E. Baum.

1. Reviews

F. J. Agee et al [1998], "Ultra-Wideband Transmitter Research," IEEE Trans. Plasma Science, pp. 860–873.

C. E. Baum [1978], "EMP Simulators for Various Types of Nuclear EMP Environments: An Interim Categorization," *IEEE Trans. Antennas and Propagation*, and *IEEE Trans. EMC*, pp. 35–53.

C. E. Baum [1992], "From the Electromagnetic Pulse to High-Power Electromagnetics," Proc. IEEE, pp. 789–817.

C. E. Baum [1997], "Transient Arrays," in C. E. Baum et al (eds.), *Ultra-Wideband, Short-Pulse Electromagnetics 3*, New York, Plenum, pp. 129–138.

C. E. Baum and E. G. Farr [1993], "Impulse Radiating Antennas," in H. Bertoni et al (eds.), *Ultra-Wideband, Short-Pulse Electromagnetics*, New York, Plenum, pp. 139–147.

E. G. Farr, C. E. Baum, and C. J. Buchenaur [1995], "Impulse Radiating Antennas, Part II," in L. Carin and L. B. Felsen (eds.), *Ultra-Wideband, Short-Pulse Electromagnetics 2*, New York, Plenum, pp. 159–170.

E. G. Farr and C. E. Baum [1997], "Impulse Radiating Antennas, Part III," in C. E. Baum et al (eds.) *Ultra-Wideband, Short-Pulse Electromagnetics 3*, New York, Plenum, pp. 43–56.

W. D. Prather et al [1997], "Ultrawide Band Source and Antennas: Present Technology, Future Challenges," in C. E. Baum et al (eds.), *Ultra-Wideband, Short Pulse Electromagnetics 3*, New York, Plenum, pp. 381–389.

I. D. Smith and H. Aslin [1978], "Pulsed Power for EMP Simulators," *IEEE Trans. Antennas and Propagation*, and *IEEE Trans. EMC*, pp. 53–59.

2. Impulse Radiating Antennas (IRAs): General

C. E. Baum [1987], “Focused Aperture Antennas,” *Sensor and Simulation Note 306*, and *Proc. 1993 Antenna Applications Symposium*, RL-TR-94-20, pp. 40–61.

C. E. Baum [1989], “Radiation of Impulse-Like Transient Fields,” *Sensor and Simulation Note* 321.

C. E. Baum [1991], “Aperture Efficiencies for IRAs,” *Sensor and Simulation Note* 328.

C. E. Baum [1997], “A Symmetry Result for an Antenna on a Truncated Ground Plane,” *Sensor and Simulation Note* 415.

C. E. Baum [1997a], “Intermediate Field of an Impulse-Radiating Antenna,” *Sensor and Simulation note* 418.

C. J. Buchenauer, J. S. Tyo, and J. S. H. Schoenberg [1997], “Aperture Efficiencies of Impulse Radiating Antennas,” *Sensor and Simulation Note 421*.

E. G. Farr and C. E. Baum [1993], “Radiation from Self-Reciprocal Apertures,” *Sensor and Simulation Note 357*, and [1995], in C. E. Baum and H. N. Kritikos (eds.), *Electromagnetic Symmetry*, Philadelphia, Taylor & Francis, pp. 281–308.

E. G. Farr and C. E. Baum [1995], “Impulse Radiating Antennas with Two Refracting Reflecting Surfaces,” *Sensor and Simulation Note* 379.

E. G. Farr and C. J. Buchenauer [1994], “Experimental Validation of IRA Models,” *Sensor and Simulation Note* 364.

E. G. Farr and C. A. Frost [1995], “Compact Ultra-Short Pulse Fuzing Antenna Design and Measurements,” *Sensor and Simulation Note* 380.

E. G. Farr and C. A. Frost [1996], “Development of a Reflector IRA and a Solid Dielectric Lens IRA, Part I: Design, predictions, and Construction,” *Sensor and Simulation Note* 396.

E. G. Farr and C. A. Frost [1996a], “Development of a Reflector IRA and a Solid Dielectric Lens IRA, Part II: Antenna Measurements and Signal processing,” *Sensor and Simulation Note* 401.

D. V. Giri, [1996], “Propagation of Impulse-Like Waveforms through the Ionosphere Modelled by a Cold Plasma,” *Theoretical Note* 366.

E. Heyman and T. Melamed [1994], “Certain Considerations in Aperture Synthesis of Ultrawideband/Short-Pulse Radiation,” *IEEE Trans. Antennas and Propagation*, pp. 518−525.

J. M. Lehr, C. E. Baum, and W. D. Prather [1997], “Fundamental Physical Considerations for Ultrafast Spark Gap Switching,” *Switching Note* 28.

S. P. Skulkin and V. I. Turchin [1994], "Radiation of Nonsinusoidal Waves by Aperture Antennas," in D. J. Serafin, J. Ch. Bolomey, and D. Dupouy (eds.), *Proc. EUROEM '94*, Bordeaux, France, pp. 1498–1504.

S. P. Skulkin [1997], "Transient Fields of Rectangular Aperture Antennas," in C. E. Baum et al (eds.), Ultra-Wideband, Short-Pulse Electromagnetics 3, New York, Plenum press, pp. 57–63.

J. S. Tyo [1998}, "Estimating the Optimum Aperture for Maximizing Prompt Aperture Efficiency in an IRA," *Sensor and Simulation Note* 422.

3. Reflector IRA

C. E. Baum [1991], "Configurations of TEM Feed for an IRA," *Sensor and Simulation Note* 327.

C. E. Baum [1997], "Some Topics Concerning Feed Arms of Reflector IRAs," *Sensor and Simulation Note* 414.

C. E. Baum [1995], "Variations on the Impulse-Radiating-Antenna Theme," *Sensor and Simulation Note* 378.

W. S. Bigelow and E. G. Farr [1997], "Design of a Feed-Point Lens with Offset Inner Conductor for a Half Reflector IRA with F/D Greater than 0.25," *Sensor and Simulation Note* 410.

W. S. Bigelow and E. G. Farr [1996], "Design Optimization of Feed-Point Lenses for Half Reflector IRAs," *Sensor and Simulation Not* 400.

L. H. Bowen and E. G. Farr [1998], "E-Field measurements for a 1 Meter Diameter Half IRA," *Sensor and Simulation Note* 419.

H.-T. Chou, P. H. Pathak, and P. R. Rousseau [1997], "Analytical Solution for Early-Time Transient Radiation from Pulse-Excited Parabolic Reflector Antennas," *IEEE Trans. Antennas and Propagation*, pp. 829–836.

C. Courtney et al [1995], "Measurement and Characterization of the Impulse Radiating Antenna," Prototype IRA Memo 5.

E. G. Farr [1991], "Analysis of the Impulse Radiating Antenna," *Sensor and Simulation Note* 329.

E. G. Farr [1993], "Optimizing the Feed Impedance of Impulse Radiating Antennas, Part I: Reflector IRAs," *Sensor and Simulation Note* 354.

E. G. Farr and C. E. Baum [1992], "Prepulse Associated with the TEM Feed of an Impulse Radiating Antenna," *Sensor and Simulation note* 337.

E. G. Farr and C. E. Baum [1993], "The Radiation Pattern of Reflector Impulse Radiating Antennas: Early-Time Response," *Sensor and Simulation Note* 358.

E. G. Farr, C. E. Baum, and W. D. Prather [1997], "Multifunction Impulse Radiating Antennas: Theory and Experiment," *Sensor and Simulation Note* 413.

E. G. Farr and G. D. Sower [1995], "Design Principles of Half Impulse Radiating Antennas," *Sensor and Simulation note* 390.

D. V. Giri [1995], "Radiated Spectra of Impulse Radiating Antennas (IRAs)," *Sensor and Simulation Note* 386.

D. V. Giri and C. E. Baum [1994], "Reflector IRA Design and Boresight Temporal Waveforms," *Sensor and Simulation Note* 365.

D. V. Giri and C. E. Baum [1997], "Temporal and Spectral Radiation on Boresight of a Reflector Type of Impulse Radiating Antenna (IRA)," in C. E. Baum et al (eds.), *Ultra-Wideband, Short-Pulse Electromagnetics* 3, New York, Plenum, pp. 65–72.

D. V. Giri and S. Y Chu [1992], "On the Low-Frequency Electric Dipole Moment of Impulse Radiating Antennas (IRA)," *Sensor and Simulation Note* 346.

D. V. Giri et al [1995], "A Reflector Antenna for Radiating Impulse-Like Waveforms," *Sensor and Simulation Note* 382.

D. V. Giri et al [1997], "Design, Fabrication, and Testing of a Paraboloidal Reflector Antenna and Pulser System for Impulse-Like Waveforms," *IEEE Trans. Plasma Science*, pp. 318–326.

O. V. Mikheev et al [1997], "New Method for Calculating Pulse Radiation from an Antenna with a Reflector," *IEEE Trans. EMC*, p. 48–54.

K. Min and M. Willis, Jr. [1997], "Dense Media Penetrating Radar," in C. E. Baum et al (eds.), *Ultra-Wideband, Short-Pulse Electromagnetics* 3, New York, Plenum press, pp. 423–430.

Y. Rahmat-Samii [1992], "Analysis of Blockage Effects on TEM-Fed Paraboloidal Reflector Antennas," *Sensor and Simulation Note* 347.

Y. Rahmat-Samii and D. W. Duan [1995], "Axial Field of a TEM-Fed UWB Reflector Antenna: PO/PTD Construction," in L. Carin and L. B. Felsen, *Ultra-Wideband, Short-Pulse Electromagnetics* 2, New York, Plenum, pp. 171–186.

Y. Rahmat-Samii and D. V. Giri [1992], "Analysis of Blockage Effects on TEM-Fed Paraboloidal Antennas (Part II: TEM Horn Illumination)," *Sensor and Simulation Note* 349.

S. P. Skulkin and V. I. Turchin [1997], "Transient Fields of Parabolic Reflector Antennas," in C. E. Baum et al (eds.), *Ultra-Wideband, Short-Pulse Electromagnetics* 3, New York, Plenum Press, pp. 81–87.

G. E. Sower et al [1998], "Design for Half Impulse Radiating Antennas: Lens material Selection and Scale-Model Testing," *Measurement Note* 54.

4. Lens IRA (Including TEM Horn)

J. F. Aurand [1997], "A TEM-Horn Antenna with Dielectric lens for Fast Impulse Response," in C. E. Baum et al (eds.), *Ultra-Wideband, Short-Pulse Electromagnetics* 3, new York, Plenum, pp. 113–120.

C. E. Baum [1995], "Low-Frequency-Compensated TEM Horn," Sensor and Simulation Note 377.

C. E. Baum [1995a], "Brewster-Angle Interface Between Flat-Plate Conical Transmission Lines," *Sensor and Simulation Note* 389.

E. G. Farr and C. E. Baum [1992], "A Simple Model of Small-Angle TEM Horns", *Sensor and Simulation Note* 340.

E. G. Farr [1994], "Off-Boresight Field of a Lens IRA," *Sensor and Simulation Note* 370.

E. G. Farr [1995], "Optimization of the Feed Impedance of Impulse Radiating Antennas, Part II: TEM Horns and Lens IRAs," *Sensor and Simulation Note* 384.

E. G. Farr, G. D. Sower, L. M. Atchley, and D. E. Ellibee [1998], "Design and Fabrication of an Ultra-Wideband High-Power Zipper Balun and Antenna," *Measurement Note* 53.

M. Kanda [1983], "Time Domain Sensors for Radiated Impulsive Measurements," *IEEE Trans. Antennas and Propagation*, pp. 438–444.

M. A. Morgan and R. Clark Robertson [1997], "Optimized TEM Horn Impulse Receiving Antenna," in C. E. Baum et al (eds.), *Ultra-Wideband, Short-Pulse Electromagnetics* 3, New York, Plenum Press, pp. 121–128.

R. C. Robertson and M. A. Morgan [1995], "Ultra-Wideband Impulse Receiving Antenna Design and Evaluation," in L. Carin and L. B. Felsen (eds.), *Ultra-Wideband, Short-Pulse Electromagnetics* 3, new York, Plenum press, pp. 179–186.

D. H. Shaubert [1977], "Measurement of the Impulse Response of Communication Antennas," *Harry Diamond Laboratories Technical Report*, HDL-TR-1832.

D. H. Shaubert, A. R. Sindoris, and F. G. Farrar [1976], "A Measurement Technique for Determining the Time-Domain Voltage Response of UHF Antennas to EMP Excitation," *Harry Diamond Laboratories Technical Report*, HDL-TR-1778.

J. S. Tyo, C. J. Buchenauer, and J. S. H. Schoenberg [1998], "Use of Isorefractive Media to Improve Prompt Aperture Efficiency in a lens IRA," IEEE Trans. Antennas and Propagation, pp. 1114–1115.

M. H. Vogel [1996], "Design of the Low-Frequency Compensation of an Extreme-Bandwidth TEM Horn and Lens IRA," *Sensor and Simulation Note* 391.

M. H. Vogel [1997], “Design of the Low-Frequency Compensation of an Extreme-Bandwidth TEM Horn and Lens IRA,” in C. E. Baum et al (eds.), *Ultra-Wideband, Short-Pulse Electromagnetics* 3, New York, Plenum Press, pp. 97–105.

J. Wells, C. E. Baum, N. Keator, and W. D. Prather [1997], “A Radiating Structure Incorporating an Extended Ground Plane and a Brewster Angle Window,” in C. E. Baum et al (eds.), *Ultra-Wideband, Short-Pulse Electromagnetics* 3, New York, Plenum press, pp. 107–112.

5. Array IRA

P. R. Barnes [1970], “Pulse Radiation by an Infinitely Long, perfectly Conducting, Cylindrical Antenna in Free Space, Excited by a Finite Cylindrical Distributed Source Specified by the Tangential Electric Field Associated with a Biconical Antenna,” *Sensor and Simulation Note* 110.

C. E. Baum [1967], “The Conical Transmission Line as a Wave Launcher and Terminator for a Cylindrical Transmission line,” *Sensor and Simulation Note* 31.

C. E. Baum [1969], “The Distributed Source for Launching Spherical Waves,” *Sensor and Simulation Note* 84.

C. E. Baum [1970], “Some Characteristics of Planar Distributed Sources for Radiating Transient Pulses,” *Sensor and Simulation Note* 100.

C. E. Baum [1972], “General Principles for the Design of ATLAS I and II, Part IV: Additional Considerations for the Design of Pulser Arrays,” *Sensor and Simulation Note* 146.

C. E. Baum [1972a], “General Principles for the Design of ATLAS I and II, part V: Some Approximate Figures of Merit for Comparing the Waveforms launched by Imperfect Pulser Arrays onto TEM Transmission Lines,” *Sensor and Simulation Note* 148.

C. E. Baum [1973], “Early Time Performance at Large Distances of Periodic Planar Arrays of Planar Bicones with Sources Triggered in a Plane-Wave Sequence,” *Sensor and Simulation Note* 184.

C. E. Baum [1988], “Coupled Transmission-Line Model of Periodic Array of Wave Launchers,” *Sensor and Simulation Note* 313.

C. E. Baum [1989], “Canonical Examples for High-Frequency Propagation on Unit Cell of Wave-Launcher Array,” *Sensor and Simulation Note* 317.

C. E. Baum [1993], “Timed Arrays for Radiating Impulse-Like Transient Fields,” *Sensor and Simulation Note* 361, and [1995], *Proc. SPIE*, Vol. 2485, pp. 168−174.

C. E. Baum [1994], “Self-Complementary Array Antennas,” *Sensor and Simulation Note* 374.

C. E. Baum and D. V. Giri [1985], “The Distributed Switch for Launching Spherical Waves,” *Sensor and Simulation Note* 289, and *Proc. 1997 EMC Symposium*, Zurich, pp. 205–212.

G. W. Carlisle [1968], "Matching the Impedance of Multiple Transitions to a Parallel-Plate Transmission Line," *Sensor and Simulation Note* 54.

Y.-G. Chen et al [1986], "Design Procedures for Arrays which Approximate a Distributed Source at the Air-Earth Interface," *Sensor and Simulation Note* 292.

Y.-G. Chen et al [1990], "Low Voltage Experiments Concerning a Section of a Pulser Array Near the Air-Earth Interface," *Sensor and Simulation Note* 322.

T. M. Flanagan et al [1987], "A Wide-Bandwidth Electric-Field Sensor for Lossy Media," *Sensor and Simulation Note* 297.

D. V. Giri [1989], "Impedance Matrix Characterization of an Incremental Length of a Periodic Array of Wave Launchers," *Sensor and Simulation Note* 316.

D. V. Giri [1989a], "A Family of Canonical Examples for High Frequency Propagation on Unit Cell of Wave-Launcher Array," *Sensor and Simulation Note* 318.

D. V. Giri and C. E. Baum [1987], "Early Time Performance at Large Distances of Periodic Arrays of Flat-Plate Conical Wave Launchers," *Sensor and Simulation Note* 299.

N. Inagaki, Y. Isogai, and Y. Mushiake [1979], "Self-Complementary Antenna with Periodic Feeding Points," *Trans. IECE*, Vol. 62-B, No. 4, pp. 388–395, in Japanese. Translation NAIC-ID(RS) T-0506-95, 1995, National Air Intelligence Center.

T. K. Liu [1973], "Admittances and Fields of a Planar Array with Sources Excited in a Plane Wave Sequence," *Sensor and Simulation Note* 186.

D. T. McGrath [1996], "Numerical Analysis of Planar Bicone Arrays," *Sensor and Simulation Note* 403.

D. T. McGrath [1998], "Numerical Analyses of TEM Horn Arrays," *Sensor and Simulation Note* 420.

Z. L. Pine and F. M. Tesche [1972], "Pulse Radiation by an Infinite Cylindrical Antenna with a Source Gap with a Uniform Field," Sensor and Simulation note 159.

6. Antenna Parameterization for Time-Domain Applications (Emphasizing Far Fields)

O. E. Allen, D. A. Hill, and A. R. Ondrejka [1993], "Time-Domain Antenna Characterizations," *IEEE Trans. EMC*, pp. 339−346.

C. E. Baum [1968], "Some Limiting Low-Frequency Characterstics of a Pulse-Radiating Antenna," *Sensor and Simulation Note* 65.

C. E. Baum [1971], "Some Characteristics of Electric and Magnetic Dipole Antennas for Radiating Transient Pulses," *Sensor and Simulation Note* 125.

C. E. Baum [1991], "General Properties of Antennas," *Sensor and Simulation Note* 330.

C. E. Baum [1995], “Optimization of Transient Radiation,” *Sensor and Simulation Note* 376.

C. E. Baum, E. G. Farr, and C. A. Frost [1997], “Transient Gain of Antennas Related to the Traditional Continuous-Wave (CW) Definition of Gain,” *Sensor and Simulation Note* 412.

E. G. Farr and C. E. Baum [1992], “Extending the Definitions of Antenna Gain and Radiation Pattern Into the Time Domain,” *Sensor and Simulation Note* 350.

D. Lamensdorf and L. Sasman [1994], “Baseband-Pulse-Antenna Techniques,” IEEE Antennas and Propagation Magazine, February, pp. 20−30.

R. E. McIntosh and J. E. Sarna [1982], “Bounds on the Optimum Performance of Planar Antennas for Pulse Radiation,"”*IEEE Trans. Antennas and Propagation*, pp. 381−389.

D. M. Pozar, D. H. Shaubert, and R. E. McIntosh [1984] “The Optimum Transient Radiation from an Arbitrary Antenna,” *IEEE Trans. Antennas and Propagation*, pp. 633−640.

A. Shlivinski, E. Heyman, and R. Kastner [1997], “Antenna Characterization in the Time Domain,” *IEEE Trans. Antennas and Propagation*, pp. 1140−1149.

F. M. Tesche [1996], “Some Considerations for the Design of Pulse-Radiating Antennas,” *Sensor and Simulation Note* 398.

A. D. Yaghjian and T. B. Hansen [1997],”Theorems on Time-Domain Far Fields,” in C. E. Baum et al (eds*.) Ultra-Wideband, Short-Pulse Electromagnetics* 3, New York, Plenum Press, pp. 165−176.

7. Transient Lenses: Approximate

C. E. Baum [1967], “A Lens Technique for Transitioning Waves Between Conical and Cylindrical Transmission Lines,” *Sensor and Simulation Note* 32.

C. E. Baum [1995], “Steerable Lens Surface for Use with the IRA Class of Antennas,” *Sensor and Simulation Note* 387.

C. E. Baum, J. J. Sadler, and A. P. Stone [1995], “A Prolate Spheroidal Uniform Dielectric Lens Feeding a Circular Coax,” *Electromagnetics*, pp. 223−241.

C. E. Baum, J. J. Sadler, and A. P Stone [1992], “Uniform Isotropic Dielectric Equal-Time Lenses for Matching Combinations of Plane and Spherical Waves,” *Sensor and Simulation Note* 352.

C. E. Baum, J. J. Sadler, and A. P. Stone [1992], “Uniform Wedge Dielectric Lenses for Bends in Circular Coaxial Transmission Lines,” *Sensor and Simulation Note* 356.

C. E. Baum, J. J. Sadler, and A. P. Stone [1993], “A Uniform Dielectric lens for launching a Spherical Wave into a Paraboloidal Reflector,” *Sensor and Simulation Note* 360.

C. E. Baum, J. J. Sadler, and A. P. Stone [1994], "Impedances of Coplanar Conical Plates in a Uniform Dielectric lens and matching Conical Plates for Feeding a Paraboloidal Reflector," *Sensor and Simulation Note* 372.

C. E. Baum, J. J. Sadler, and A. P. Stone [1997], "Coplanar Conical Plates in a Uniform Dielectric Lens with Matching Conical Plates for Feeding a Paraboloidal Reflector," in C. E. Baum et al (eds.) *Ultra-Wideband Short-Pulse Electromagnetics* 3, New York, Plenum Press, pp. 73−80.

E. G. Farr and C. E. Baum [1995], "Feed-Point Senses for Half Reflector IRAs," *Sensor and Simulation Note* 385.

8. Transient Lenses: Exact

W. S. Bigelow and E. G. Farr [1998], "Minimizing Dispersion in a TEM Waveguide Bend by a Layered Approximation of a Graded Dielectric Material," *Sensor and Simulation Note* 416.

C. E. Baum [1991], "Wedge Dielectric Lenses for TEM Waves Between Parallel Plates," *Sensor and Simulation Note* 332.

C. E. Baum [1992], "Arrays of Parallel Conducting Sheets for Two-Dimensional E-Plane Bending lenses," *Sensor and Simulation Note* 341.

C. E. Baum [1995], "Two-Dimensional Inhomogeneous Dielectric Lenses for E-Plane Bends of TEM Waves Guided Between Perfectly Conducting Sheets," *Sensor and Simulation Note* 388.

C. E. Baum [1996], "Dielectric Body-of-Revolution Lenses with Azimuthal Propagation," *Sensor and Simulation Note* 393.

C. E. Baum [1996a], "Dielectric Jackets as Lenses and Application to Generalized Coaxes and Bends in Coaxial Cables," *Sensor and Simulation Note* 394.

C. E. Baum [1996b], "Azimuthal TEM Waveguides in Dielectric Media," Sensor and Simulation Note 397.

C. E. Baum [1996c], "Discrete and Continuous E-Plane Bends in Parallel-Plate Waveguide," Sensor and Simulation Note 399.

C. E. Baum [1996d], "Use of Generalized Inhomogeneous TEM Plane Waves in Differential Geometric Lens Synthesis," *Sensor and Simulation Note* 405, and *Proc. 1998 International Symposium on Electromagnetic Theory*, Thessaloniki, Greece, pp. 636−638.

C. E. Baum and A. P. Stone [1991], *Transient Lens Synthesis: Differential Geometry in Electromagnetic Theory*, Philadelphia, Taylor & Francis.

C. E. Baum and A. P. Stone [1993], "Transient Lenses for Transmission Systems and Antennas," in H. Bertoni et al (eds.), *Ultra-Wideband, Short-Pulse Electromagnetics*, New York, Plenum Press, pp. 211−219.

C. E. Baum and A. P. Stone [in publication], "Synthesis of Purely Dielectric Transient Lenses," in *Ultra-Wideband, Short-Pulse Electromagnetics* 4, New York, Plenum Press.

9. Fields from Circular-Disk Sources Focused at Infinity

C. E. Baum [1992], "Circular Aperture Antennas in Time Domain," *Sensor and Simulation Note* 351.

D. J. Blejer [1989], "On-Axis Transient Fields from a Uniform Circular Distribution of Electric or Magnetic Current," PIERS Proc., pp. 362−363.

D. J. Blejer, R. C. Wittmann, and A. D. Yaghjian [1993], "On-Axis Fields From a Circular Uniform Surface Current," in H. Bertoni et al (eds.), *Ultra-Wideband, Short-Pulse Electromagnetics*, New York, Plenum, pp. 285−292.

R. R. Rudduck and C.-L. Chen [1976], "New Plane Wave Spectrum Formulations for the Near-Fields of Circular and Strip Antennas," *IEEE Trans. Antennas and Propagation*, pp. 438−449.

A. D. Yaghjian [1982], "Eficient Computation of Antenna Coupling and Fields Within the Near-Field Region," *IEEE Trans. Antennas and Propagation*, pp. 113−128.

10. Related Matter: Special Kinds of Waves (Selected)

J. L. Brittingham [1983], "Focus Waves Modes in Homogeneous Maxwell's Equations: Transverse Electric Mode," *J. Appl. Phys*., pp. 1179−1189.

B. B. Godfrey [1989], "Diffraction-Free Microwave Propagation," *Sensor and Simulation Note* 320.

E. Heyman [1993], "Wavepacket Solutions of the Time-Dependent Wave Equation in Homogeneous and Inhomogeneous Media," in H. Bertoni et al (eds.), *Ultra-Wideband, Short-Pulse Electromagnetics*, New York, Plenum Press, pp. 241−250.

E. Heyman and L. B. Felsen [1986], "Propagating Pulsed Beam Solutions by Complex Source Parameter Substitution," *IEEE Trans. Antennas and Propagation*, pp. 1062−1065.

H. E. Moser and R. T. Prosser [1986], "Initial Conditions, Sources, and Currents for Prescribed Time-Dependent Acoustic and Electromagnetic Fields in three Dimensions, part I: The Inverse Initial Value Problem. Acoustic and Electromagnetic "Bullets,' Expanding Waves, and Imploding Waves," *IEEE Trans. Antennas and Propagation*, pp. 188-196.

T. T. Wu [1985], "Electromagnetic Missiles," J. Appl. Phys., pp. 2370−2375.

J. Zhan [1990], "General and Sufficient Electromagnetic Missile Condition," *IEEE Trans. EMC*, pp. 304−307.

R. W. Ziolkowski [1992], "Properties of Electromagnetic Beams Generated by Ultra-Wide Bandwidth Pulse-Driven Arrays," *IEEE Trans. Antennas and Propagation*, pp. 888−905.

R. W. Ziolkowski [1993], "UltraWide Bandwidth, Multi-Derivative Electromagnetic Systems," in H. Bertoni et al (eds.), *Ultra-Wideband, Short-Pulse Electromagnetics*, New York, Plenum Press, pp. 251−258.